

# Pre-clinical characterization of monoclonal antibodies targeting CD39 activity in the acidic tumor microenvironment



F. Donelson Smith, Arnab Mukherjee, Yuliya Kleschenko, Adejumo Onumajuru, Zuzana Biesova, Vikas Saxena, Thomas Thisted, and Edward H. van der Horst

Sensei Biotherapeutics Inc., 1405 Research Blvd, Suite 125, Rockville, MD 20850

Poster 195-A

## Introduction

CD39 (ENTPD1) expression is upregulated on various cell types, including lymphocytes and myeloid cells, within the tumor microenvironment (TME), a niche that is characterized by high extracellular ATP (eATP) levels and low pH. CD39 catalyzes the rate-limiting degradation step of eATP to AMP prior to its conversion to adenosine, a signaling molecule that promotes an immunosuppressive state, impairing anti-tumor T-cell function<sup>1</sup>. CD39 inhibition presents a potential novel immunotherapeutic approach, but the broad expression of CD39 on endothelial cells and macrophages poses significant pharmacokinetic challenges<sup>2</sup>.

Our strategy targets CD39 activity selectively within the TME to restore the immunostimulatory environment while avoiding pharmacokinetic issues<sup>3</sup>. We discovered pH-selective anti-CD39 antibodies with potent anti-tumor activity *in vivo*, and characterized optimized progeny mAbs using *in vitro* activity assays, *in vivo* pharmacokinetics, structural determination, and computational modeling.

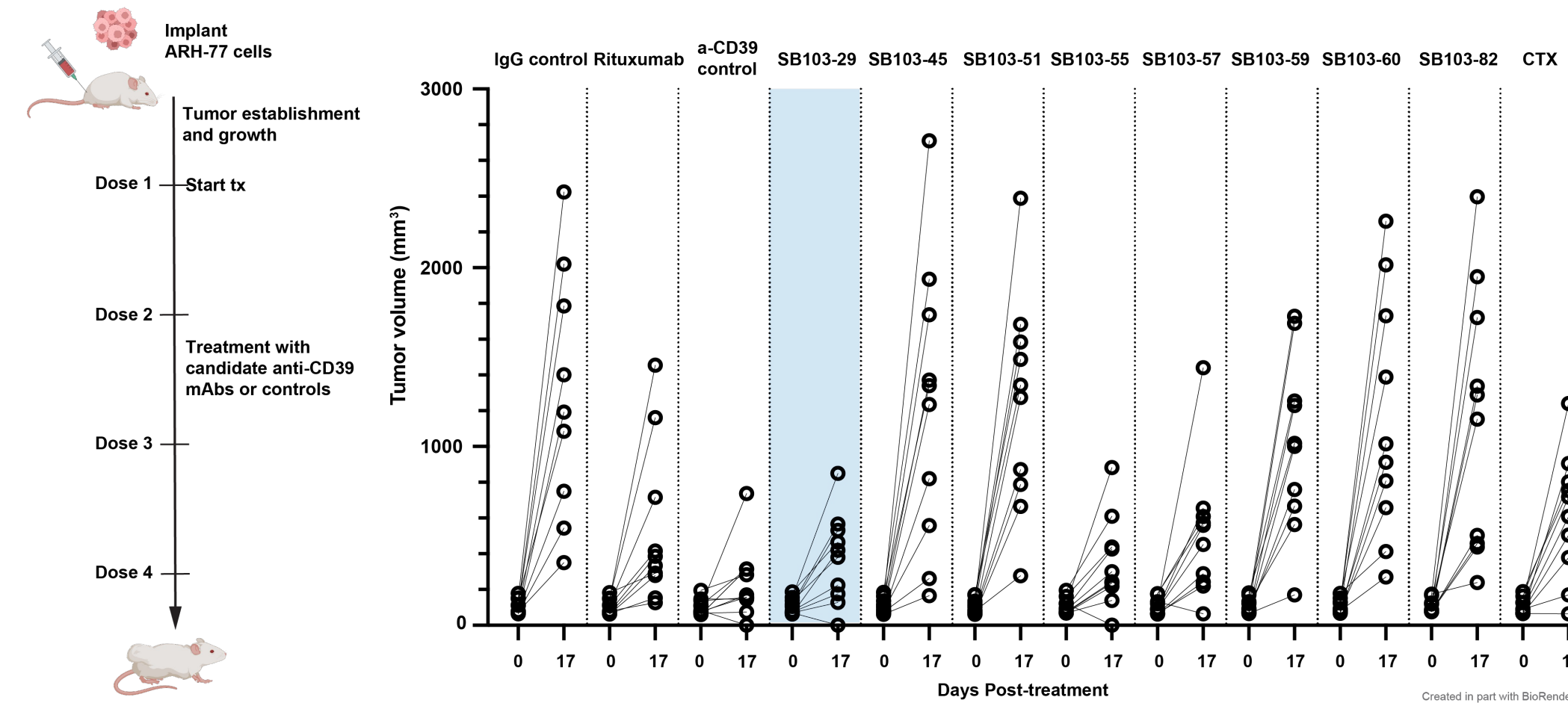


**Figure 2. Anti-tumor activity of anti-CD39 antibodies**

Eight candidate anti-CD39 mAbs were tested for efficacy in controlling ARH-77 tumors in congenic SCID mice (n=12/group). Cells were implanted subcutaneously and allowed to establish ~70-100 mm<sup>3</sup> tumors prior to start of treatment. IgG isotype matched mAbs were used as negative controls. Rituximab, cyclophosphamide (CTX) and a published inhibitory anti-CD39 mAb were used as controls. Antibodies were dosed at 15 mg/kg; CTX was dosed at 125 mg/kg. Individual tumor volumes are displayed for start of treatment and at day 17 post-treatment initiation.

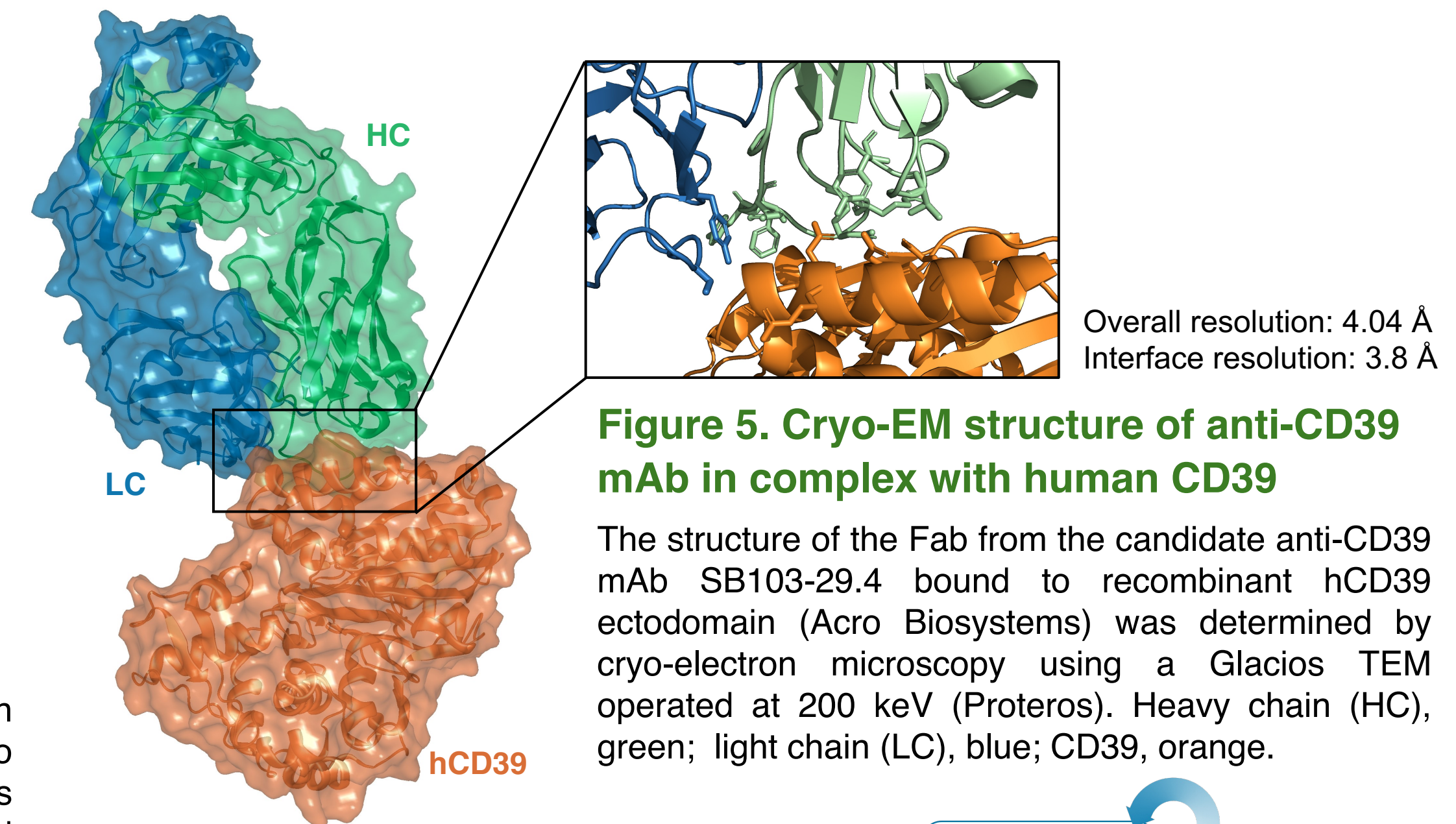


**Figure 5. Cryo-EM structure of anti-CD39 mAb in complex with human CD39**

The structure of the Fab from the candidate anti-CD39 mAb SB103-29.4 bound to recombinant hCD39 ectodomain (Acro Biosystems) was determined by cryo-electron microscopy using a Glacios TEM operated at 200 keV (Proteros). Heavy chain (HC), green; light chain (LC), blue; CD39, orange.

## Workflow for modeling and development of variants with enhanced pH selectivity

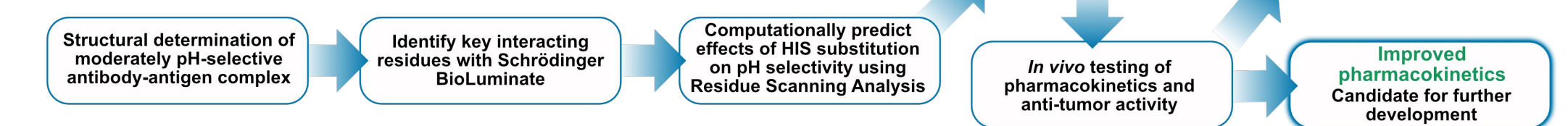


## Figure 3. Improved properties of 2<sup>nd</sup> generation anti-CD39 mAbs

Lead optimization of SB103-29 led to progeny antibodies with (A) higher affinity for CD39 and (B) stronger inhibition of enzymatic activity at pH 6.0. A single candidate (SB103-29.4, orange) was chosen for further development.

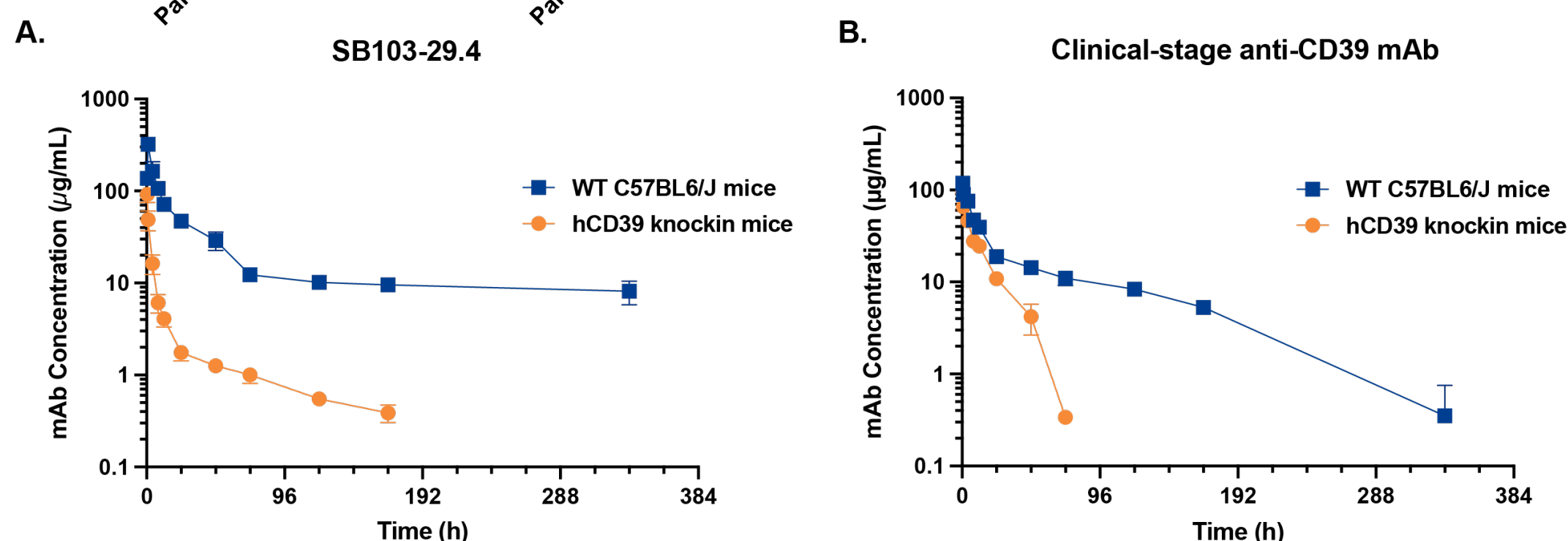
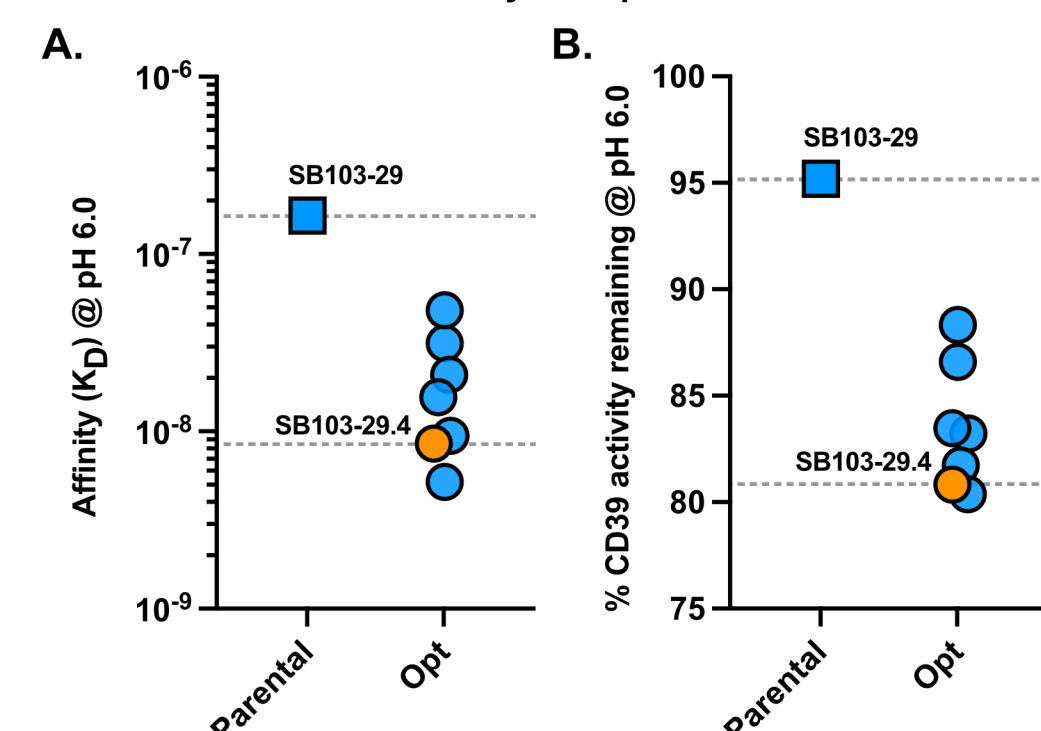


**Figure 4. Pharmacokinetic analysis of anti-CD39 mAbs**

Pharmacokinetic analysis was performed by a single dose injection (5 mg/kg I.V.) of mAb into either WT C57BL/6 mice or human CD39-knockin mice (Genoway). Serum was analyzed at 11 time points post-administration. (A) The second generation anti-CD39 mAb SB103-29.4. (B) A clinical-stage inhibitory anti-CD39 mAb was used as a comparator. SB103-29.4 displays a biphasic pharmacokinetic profile indicative of a fast equilibration phase followed by slow elimination, as well as decreased target-mediated drug disposition, as compared to a clinical stage comparator anti-CD39 mAb.

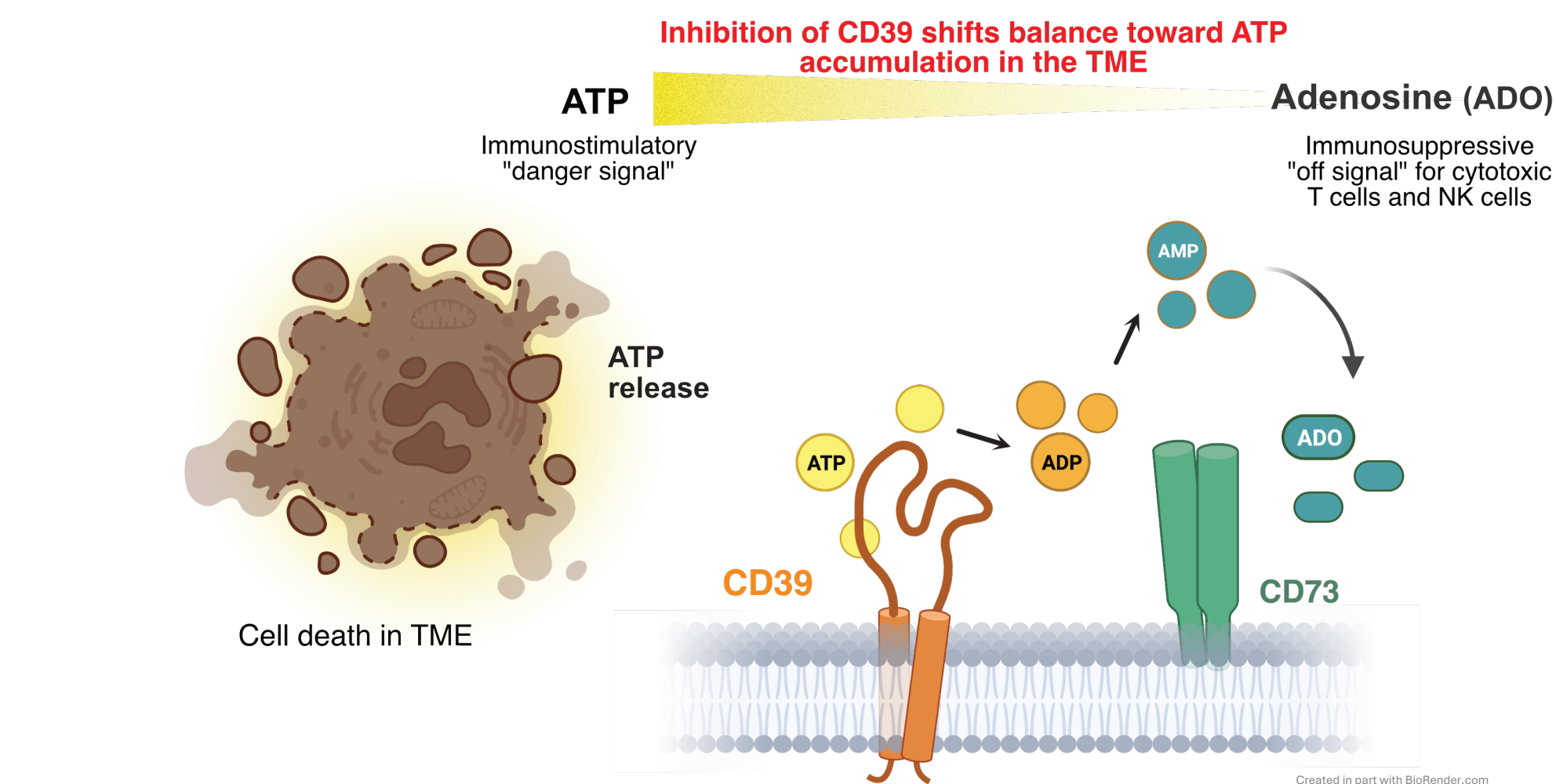


**Figure 1. CD39 function in the tumor microenvironment**

Cell death in the tumor microenvironment results in release of immunostimulatory ATP into the extracellular space. CD39 metabolizes ATP to ADP and AMP, which is then degraded to the immunosuppressive molecule adenosine by CD73. Inhibition of CD39 in the TME results in accumulation of ATP and a decrease in adenosine favoring immune activity and tumor cell killing. High eATP may also have direct effects on tumor cell survival.

## Methods

Anti-CD39 antibodies were discovered and optimized through a yeast-based screening platform. Candidates were tested for binding to CD39-expressing cells using flow cytometry and for inhibition of CD39 activity *in vitro* using recombinant CD39 and CD39-positive cell lines<sup>3</sup>. Pharmacokinetics and tumor growth inhibition were assessed *in vivo*. Cryo-electron microscopy was performed with a lead Fab-antigen complex. Computational modeling was performed using Schrödinger Biologics BioLuminate software, and *in vitro* binding was measured on a Bruker Sierra SPR-24 Pro instrument.

Variant #	COMPUTATIONAL			EXPERIMENTAL		
	Δ Affinity pH 5.0 (kcal/mol)	Δ Affinity pH 7.4 (kcal/mol)	Difference pH 5.0 – pH 7.4	K <sub>D</sub> pH 6.0 (nM)	K <sub>D</sub> pH 7.4 (nM)	Ratio pH 7.4/pH 6.0
WT	–	–	–	0.9	12	13.3
1	-7.72	-1.75	-5.99	TBD	TBD	–
2	6.41	11.3	-4.87	TBD	TBD	–
3	-3.90	3.96	-7.86	4.9	149	30.4
4	-8.41	0.89	-9.29	1.2	14	11.7
5	-0.71	2.44	-3.15	4	39	9.8
6	-0.32	-1.65	1.33	7.6	63	8.3
7	0.39	1.86	-1.47	1.2	80	66.6
8	19.0	41.9	-22.9	8	178	22.3
9	-10.9	4.8	-15.7	3.9	190	48.7
10	-7.96	-12.5	4.57	0.17	6.2	36.5

**Table 1. Computationally derived variants for enhanced pH selectivity**

Computational modeling was performed to predict changes in binding energies upon histidine substitution of interacting residues within antibody CDRs. Variant mAbs were expressed and purified from mammalian cells and tested for binding to purified hCD39 ectodomain by SPR.

## Conclusions

- Screening under low-pH selection conditions yielded inhibitory anti-CD39 antibodies with anti-tumor activity *in vivo*. Additional rounds of selection improved affinity, and pH dependence.
- A lead candidate with strong anti-tumor activity demonstrates favorable pharmacokinetic properties.
- Structural determination by cryo-EM identified the epitope on CD39.
- Computational modeling identifies variants with improved pH-selectivity while maintaining high affinity and inhibitory activity. Select variants will be tested *in vivo* for improvements in PK and tumor control.